13th International Symposium on Turbulence and Shear Flow Phenomena (TSFP13)
Montreal, Canada, June 25–28, 2024

HELICAL TURBULENCE - THE TRANSITION BETWEEN 2D AND 3D TURBULENCE

Schahin Akbari, Martin Oberlack
Department of Mechanical Engineering
TU Darmstadt
Otto-Bernd-Str. 2, 64287 Darmstadt, Germany
akbari@fdy.tu-darmstadt.de

ABSTRACT

Based on vortex stretching, our theoretical understanding of 2D and 3D turbulence reveals fundamental differences. To gain further insights, we study helically-symmetric flows, which allow to study precisely this transition between 2D and 3D turbulence. The helical coordinate system is represented by it's direction r, $\xi = az + b\phi$ and $\eta = -bz + ar^2\phi$, where $a, b = \text{const}$, $a^2 + b^2 > 0$ and (r, ϕ, z) are cylindrical coordinates.

Helical symmetry is defined by η-independent flow-variables, thus $\partial/\partial\eta \equiv 0$ holds for all dependent variables. Helical flows significantly differ based on whether they have a velocity u^η along the helical coordinate ξ. For $u^\eta = 0$ vortex stretching is switched off while for $u^\eta \neq 0$ vortex stretching is active even though all flow variables only live on the 2D (r, ξ)-manifold. In both cases, helical flows possess infinite classes of conservation laws (CL), and thus related, integral invariants. For $u^\eta \neq 0$ the central new invariants result from an infinite set of generalized helicity CL, and for $u^\eta = 0$ we find infinitly many generalized enstrophy CL (Kelbin *et al.*, 2013). Our knowledge about 2D and 3D turbulence reveals that local and global invariants play a central role in turbulence and this we also observe for helical turbulence.

For helical flows with vortex stretching, as in the general 3D case, we expect the anomalous scaling of dissipation for the limit $\nu \to 0$ and the resulting Kolmogorov scaling. On the other hand, the helicity cascade and its scaling will depend on which of the global helicity invariants one chooses as initial condition. The case without vortex stretching is closer to the 2D case and different new energy spectra arise for limiting cases $r \to 0$ and $r \to \infty$.

Additionally, the transition from 2D to 3D turbulence is investigated by analyzing asymptotically small vortex stretching, i.e. $u^\eta \ll 1$. This allows to also theoretically trace the transition between the two cases above using the method of approximate CL. Results and comparison of invariant theory and high-fidelity simulation of helical turbulence will be presented at the meeting.

HELICAL FLOWS IN SCIENCE & TECHNOLOGY

Helical flow structures appear in various natural phenomena and technological devices, for example, in the wake of windmills (Vermeer *et al.*, 2003), as wing tip vortices (Mitchell *et al.*, 2002), and in rotor-induced flows where instabilities can lead to vortex pairing (Abraham *et al.*, 2023). They also occur in astrophysical plasmas (Bogoyavlenskij, 2000) and in laboratory experiments such as "straight tokamak" plasma flow approximations (see e.g. Schnack *et al.* (1985); Johnson *et al.* (1958)). In particular, helical vortex structures were observed by Sarpkaya (1971) in experiments with swirling flows in a cylindrical tube, and as such, they are part of the various flow structures observed in the known phenomena of vortex breakdown. Using non-orthogonal and local-orthogonal coordinate systems, the effects of pipe curvature and torsion on the flow were investigated. Special analytical solutions of steady flows in helically symmetric pipes were found by Zabielski & Mestel (1998). Delbende *et al.* (2012) has developed a DNS code for the helical invariant Navier-Stokes equations (NSE) in a generalized vorticity-streamfunction formulation. Dritschel (1991) reduced the three-dimensional Euler equations to a linear equation, assuming that the flow has helical symmetry and consists of a rigidly rotating basic part and a Beltrami disturbance part. In the study by Kelbin *et al.* (2013), CLs for fluid flows with helical symmetry are explored. Dierkes *et al.* (2021) developed a high-order discontinuous Galerkin scheme tailored for these helically symmetric NSE. This method is no-

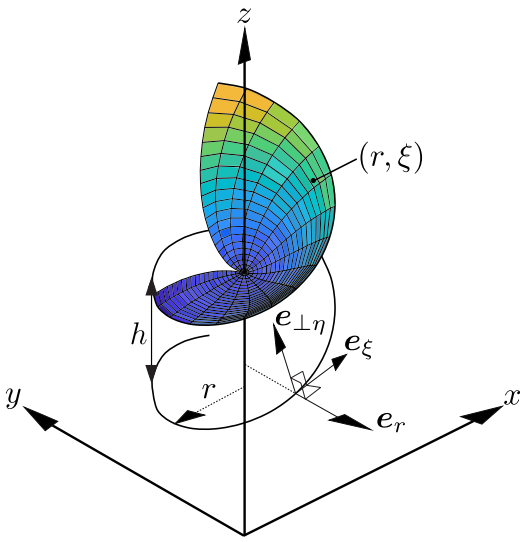

Figure 1. Helical flows live on a 2D manifold (r, ξ) embedded in a 3D space. For illustration, the outer helix shows a line of varying ξ and constant r. h represents the pitch of the helix. On the (r, ξ)-surface all flow variables are defined, i.e. pressure, vorticity and velocity and the last two denote vectors which have three independent components.

table for its discretization technique, attention to the central axis, and a semi-explicit temporal integration strategy, all designed to ensure the theoretical convergence rates across the computational domain, including areas near the central axis.

HELICAL SYMMETRIC NAVIER STOKES EQN

To derive the governing equations within a helically symmetric framework, one begins with the symbolic form of the NSE for an incompressible fluid

$$\begin{aligned} \nabla \cdot \boldsymbol{u} &= 0, \\ \frac{\mathrm{d}\boldsymbol{u}}{\mathrm{d}t} \equiv \left(\frac{\partial \boldsymbol{u}}{\partial t} + \boldsymbol{u} \cdot \nabla \boldsymbol{u} \right) &= -\frac{1}{\rho} \nabla p + \nu \nabla^2 \boldsymbol{u}. \end{aligned} \tag{1}$$

To accurately describe the helically symmetric motion, one needs two new helical variables, ξ and η, which are defined by

$$\xi = az + b\phi, \qquad \eta = -bz + ar^2\phi, \tag{2}$$

where a, $b =$ are const, $a^2 + b^2 > 0$ and (r, ϕ, z) are the common cylindrical coordinates. We express the velocity vector using helical basis vectors (as shown in figure 1)

$$\boldsymbol{u} = u^r \, \boldsymbol{e}_r + u^\eta \, \boldsymbol{e}_{\perp\eta} + u^\xi \, \boldsymbol{e}_\xi. \tag{3}$$

Considering the helical symmetry, characterized by the condition $\partial/\partial\eta \equiv 0$, and utilizing the previously defined variables ξ and η, the NSE can be reformulated as

$$\frac{1}{r}\left(r\,u^r\right)_r + \frac{1}{B}(u^\xi)_\xi = 0, \tag{4a}$$

$$\begin{aligned} &(u^r)_t + u^r(u^r)_r + \frac{1}{B}u^\xi(u^r)_\xi - \frac{B^2}{r}\left(\frac{b}{r}u^\xi + a u^\eta\right)^2 = \\ &-p_r + \nu\left[\frac{1}{r}\left(r(u^r)_r\right)_r + \frac{1}{B^2}(u^r)_{\xi\xi} - \frac{1}{r^2}u^r - \frac{2\,b\,B}{r^2}\left(a(u^\eta)_\xi + \frac{b}{r}(u^\xi)_\xi\right)\right], \end{aligned} \tag{4b}$$

$$\begin{aligned} &(u^\eta)_t + u^r(u^\eta)_r + \frac{1}{B}u^\xi(u^\eta)_\xi + \frac{a^2B^2}{r}u^r u^\eta = \\ &\nu\left[\frac{1}{r}\left(r(u^\eta)_r\right)_r + \frac{1}{B^2}(u^\eta)_{\xi\xi} + \frac{a^2B^2(a^2B^2-2)}{r^2}u^\eta + \frac{2\,a\,b\,B}{r^2}\left((u^r)_\xi - (Bu^\xi)_r\right)\right], \end{aligned} \tag{4c}$$

$$\begin{aligned} &(u^\xi)_t + u^r(u^\xi)_r + \frac{1}{B}u^\xi(u^\xi)_\xi + \frac{2\,a\,b\,B^2}{r^2}u^r u^\eta + \frac{b^2B^2}{r^3}u^r u^\xi = \\ &-\frac{1}{B}p_\xi + \nu\left[\frac{1}{r}\left(r(u^\xi)_r\right)_r + \frac{1}{B^2}(u^\xi)_{\xi\xi} + \frac{a^4B^4-1}{r^2}u^\xi + \frac{2\,b\,B}{r^2}\left(\frac{b}{r^2}(u^r)_\xi + \frac{a\,B}{r}(u^\eta)_r\right)\right], \end{aligned} \tag{4d}$$

with $B = \frac{r}{\sqrt{a^2\,r^2+b^2}}$ (Kelbin *et al.*, 2013). We observe that all three velocity components (u^r, u^η, u^ξ) may be non-zero and evolve on a 2D (r,ζ)-manifold (see figure 1). By taking the curl of the Navier-Stokes Equations (1) and introducing the vorticity vector $\boldsymbol{\omega} = \nabla \times \boldsymbol{u}$, one obtains the vorticity transport equation

$$\frac{\mathrm{d}\boldsymbol{\omega}}{\mathrm{d}t} \equiv \frac{\partial \boldsymbol{\omega}}{\partial t} + (\boldsymbol{u} \cdot \nabla)\boldsymbol{\omega} = (\boldsymbol{\omega} \cdot \nabla)\boldsymbol{u} + \nu \nabla^2 \boldsymbol{\omega}. \tag{5}$$

The term $(\boldsymbol{\omega}\cdot\nabla)\boldsymbol{u}$ represents the vortex stretching term, which is a key mechanism in the dynamics of turbulent flows.

CONSERVATION LAWS

The governing principles in fluid mechanics are the CL for mass, momentum, and energy (Kundu *et al.*, 2011). A local CL is a divergence expression

$$\frac{\partial \Theta}{\partial t} + \nabla \cdot \boldsymbol{\Phi} = 0; \tag{6}$$

where Θ is the density and components of $\boldsymbol{\Phi}$ are spatial fluxes. An important class of CL in fluid dynamics are the material CL given by vanishing material derivatives

$$\frac{d\Theta}{dt} \equiv \frac{\partial \Theta}{\partial t} + \boldsymbol{u} \cdot \nabla \Theta = 0. \tag{7}$$

If (7) holds, the total amount of the quantity Θ initially assigned to any fluid parcel is conserved for all times.

Classical Conservation Laws

Below are classical illustrative examples of these conservation principles, which are of interest in the further analysis. We distinguish between a thee-dimensional $\boldsymbol{u} = (u^x, u^y, u^z)$ and a two-dimensional $\boldsymbol{u} = (u^x, u^y, 0)$ flow.

3D Flow The helicity H of a given domain V of an inviscid fluid is constant and defined as

$$H = \int_V h \, d\boldsymbol{V} = const, \tag{8}$$

with $h \equiv \boldsymbol{u} \cdot \boldsymbol{\omega}$ as the local helicity. If the vortex lines are closed in V, then H is an invariant of the motion (Davidson,

2004). One can show that the local helicity h is conserved by applying the chain rule $\frac{\mathrm{d}h}{\mathrm{d}t} = \frac{\mathrm{d}(\boldsymbol{u}\cdot\boldsymbol{\omega})}{\mathrm{d}t} = \boldsymbol{u}\cdot\frac{\mathrm{d}\boldsymbol{\omega}}{\mathrm{d}t} + \boldsymbol{\omega}\cdot\frac{\mathrm{d}\boldsymbol{u}}{\mathrm{d}t}$. By inserting the definition of the rate of change of velocity, $\mathrm{d}\boldsymbol{u}/\mathrm{d}t$, from equation (1), and the rate of change of vorticity, $\mathrm{d}\boldsymbol{\omega}/\mathrm{d}t$, from equation (5), assuming a zero viscosity ($\nu = 0$) and further employing certain tensor identities, we obtain the divergence form of helicity conservation

$$\frac{\partial h}{\partial t} + \nabla\cdot(\boldsymbol{u}\times\nabla E + (\boldsymbol{\omega}\times\boldsymbol{u})\times\boldsymbol{u}) = 0, \tag{9}$$

where the total energy dencity E is defined as $E = \frac{1}{2}|\boldsymbol{u}|^2 + p$.

2D Flow For two-dimensional flow, an illustrative example of a conserved material quantity is the enstrophy Z. Considering the definition of two-dimensional flow, where the velocity field is given by $\boldsymbol{u} = (u^x, u^y, 0)$ and the vorticity vector by $\boldsymbol{\omega} = (0, 0, \omega^z)$, the vorticity transport equation (referenced as equation (5)) simplifies significantly. In such a scenario, the equation reduces to

$$\frac{\mathrm{d}\omega^z}{\mathrm{d}t} = \frac{\partial\omega^z}{\partial t} + \boldsymbol{u}\cdot\nabla\omega^z = \nu\,\Delta\omega^z. \tag{10}$$

When multiplied by the arbitrary function $\mathcal{F}'(\omega^z)$, and further assuming $\nu = 0$, an infinite number of CLs are obtained

$$\frac{\mathrm{d}\mathcal{F}(\omega^z)}{\mathrm{d}t} = \frac{\partial\mathcal{F}(\omega^z)}{\partial t} + \boldsymbol{u}\cdot\nabla\mathcal{F}(\omega^z) = 0. \tag{11}$$

Assuming e.g. $\mathcal{F}(\omega^z) = \frac{1}{2}(\omega^z)^2$, we obtain the classical example of Enstrophy conservation, and hence we get

$$Z = \frac{1}{2}\int_V \omega^2 d\boldsymbol{A} = const. \tag{12}$$

Conservation Laws for helically symmetric flows

As in the classical 2D-3D framework, we distinguish two cases within the helical framework, where for both an infinity set of CLs is obtained. The distinction is made on the basis of u^η, i.e. whether it is zero or non-zero.

$u_\eta \neq 0$: If the u^η velocity along the helix is non-zero a family of generalized helicity CL have been found (Kelbin *et al.*, 2013). From the equation (4) and (14) we may derive an infinite number of generalized helicity CL, which read

$$\left(h\,\mathcal{H}\left(\frac{r}{B}u^\eta\right)\right)_t + \nabla\cdot\left[\mathcal{H}\left(\frac{r}{B}u^\eta\right)[\boldsymbol{u}\times\nabla E + (\boldsymbol{\omega}\times\boldsymbol{u})\times\boldsymbol{u}] + E u^\eta \boldsymbol{e}_{\perp\eta}\times\nabla\mathcal{H}\left(\frac{r}{B}u^\eta\right)\right] = 0, \tag{13}$$

where $\mathcal{H}(\cdot)$ is an arbitrary function of its argument. $\mathcal{H} = 1$ inserted into (13) refers to the usual helicity CL (9). It should be noted at this point in particular that this conservation law represents the only infinite-dimensional CL in which the conserved quantity, i.e. the density, does not represent a materially conserved quantity in the sense of equation (7).

$u_\eta = 0$: In helical form, the general vorticity transport equation reads

$$(\omega^r)_t + u^r(\omega^r)_r + \frac{u^\xi}{B}(\omega^r)_\xi = \omega^r(u^r)_r + \frac{\omega^\xi}{B}(u^r)_\xi + \nu\left[\frac{1}{r}(r(\omega^r)_r)_r + \frac{1}{B^2}(\omega^r)_{\xi\xi} - \frac{1}{r^2}\omega^r - \frac{2\,b\,B}{r^2}(a\,(\omega^\eta)_\xi + \frac{b}{r}(\omega^\xi)_\xi)\right], \tag{14a}$$

$$(\omega^\eta)_t + u^r(\omega^\eta)_r + \frac{u^\xi}{B}(\omega^\eta)_\xi - \frac{a^2B^2}{r}(u^r\omega^\eta - u^\eta\omega^r) + \frac{2\,a\,b\,B^2}{r^2}(u^\xi\omega^r - u^r\omega^\xi) = \omega^r(u^\eta)_r + \frac{\omega^\xi}{B}(\partial u^\eta)_\xi + \nu\left[\frac{1}{r}(r(\omega^r)_r)_r + \frac{1}{B^2}(\omega^\eta)_{\xi\xi} + \frac{a^2B^2(a^2B^2-2)}{r^2}\omega^\eta + \frac{2\,a\,b\,B}{r^2}\left((\omega^r)_\xi - (B\omega^\xi)_r\right)\right], \tag{14b}$$

$$(\omega^\xi)_t + u^r(\omega^\xi)_r + \frac{u^\xi}{B}(\omega^\xi)_\xi + \frac{1-a^2B^2}{r}(u^\xi\omega^r - u^r\omega^\xi) = \omega^r(u^\xi)_r + \frac{\omega^\xi}{B}(u^\xi)_\xi + \nu\left[\frac{1}{r}\left(r(\omega^\xi)_r\right)_r + \frac{1}{B^2}(\omega^\xi)_{\xi\xi} + \frac{a^4B^4-1}{r^2}\omega^\xi + \frac{2\,b\,B}{r^2}\left(\frac{b}{r^2}(\omega^r)_\xi + \frac{a\,B}{r}(\omega^\eta)_r\right)\right], \tag{14c}$$

where the first two terms on the right-hand side of each equation correspond to vortex stretching. For the case $u_\eta = 0$, the vortex stretching terms in (14) all vanish, and further the two vorticity components vanish identically, i.e.

$$\omega^r = \frac{1}{B}(u^\eta)_\xi = 0, \tag{15}$$

and

$$\omega^\xi = (u^\eta)_r + \frac{a^2\,B^2}{r}u^\eta = 0. \tag{16}$$

Consequently, the corresponding equations also disappear identically. Moreover, the remaining vorticity component ω^η

is aligned with the helix, which can be expressed as

$$\omega^\eta = \frac{1}{B}\left(u^r\right)_\xi - \frac{1}{r}\left(r u^\xi\right)_r + \frac{a^2 B^2}{r} u^\xi. \tag{17}$$

The ω^η-vorticity equation in (14b) then reduces to

$$\begin{aligned}&(\omega^\eta)_t + u^r\,(\omega^\eta)_r + \frac{1}{B}u^\xi(\omega^\eta)_\xi - \frac{a^2B^2}{r}(u^r\omega^\eta) = \\ &\nu\left[\frac{1}{r}\left(r(\omega^\eta)_r\right)_r + \frac{1}{B^2}(\omega^\eta)_{\xi\xi} + \frac{a^2B^2\left(a^2\,B^2-2\right)}{r^2}\omega^\eta\right].\end{aligned} \tag{18}$$

To understand the enstrophy dynamics of helically symmetric turbulence in the limit of $u^\eta = 0$, equation (19) is multiplied by $\omega^\eta\, B^2/r^2$ before taking the ensemble average. Assuming statistical homogeneity, we find that all divergences integrate to zero, leading to

$$\begin{aligned}&\frac{\mathrm{d}}{\mathrm{d}t}\left[\frac{1}{2}\left\langle\left(\omega^{\mathrm{Z}}\right)^2\right\rangle\right] = -\overbrace{\nu\left[\left\langle\ell\left(\omega^{\mathrm{Z}}\right)^2\right\rangle + \left\langle\left(\nabla\left(\omega^{\mathrm{Z}}\right)\right)^2\right\rangle\right]}^{\zeta} \\ &\text{with}\quad \ell = \frac{2\,a^2\,b^2\,B^4}{r^4}\quad\text{and}\quad \omega^{\mathrm{Z}} = \left(\frac{B}{r}\omega^\eta\right),\end{aligned} \tag{19}$$

where $\langle\cdot\rangle$ denoted as ensemble average and ζ is the enstrophy flux. We note that in the present helical system, we have in equation (19) the additional term $\langle\ell(\omega^Z)^2\rangle$, which together with the last term defines the helical enstrophy flux ζ, and this is clearly different from the classical Cartesian setting. Similar to 2D flows in equation (11), an infinite set of Enstrophy-type conservation laws can be constructed for the present helically symmetric flow. For this we set in equation (14b) $\nu = 0$, and multiply it with $\mathcal{G}'\left(\frac{B}{r}\omega^\eta\right)\frac{B}{r}$ and obtain an infinite number of material CLs similar to equation (7) (see Kelbin *et al.* (2013)). After integrating accordingly, we obtain

$$Z_{\mathcal{G}} = \int_D \mathcal{G}\left(\frac{B}{r}\omega^\eta\right) d\boldsymbol{A}, \tag{20}$$

which denotes the helical Enstrophy for $\mathcal{G}(\cdot) = (\cdot)^2$ where B is as previously defined. Here, $d\boldsymbol{A}$ is defined by $d\boldsymbol{A} = 1\, dr\, d\xi$.

ENERGY SPECTRA

In the context of turbulence, the energy spectrum usually, denoted as $E(k)$, represents the distribution of kinetic energy in turbulent flow across various wavenumbers k. These wavenumbers are inversely proportional to the size of the eddies or turbulent structures.

Energy Spectra in Cartesian Coordinates

It is essential to distinguish between three-dimensional $\boldsymbol{u} = (u^x, u^y, u^z)$ and two-dimensional $\boldsymbol{u} = (u^x, u^y, 0)$ turbulence, as the dimensionality critically influences the distributions, cascades and dynamics of kinetic energy in turbulent systems.

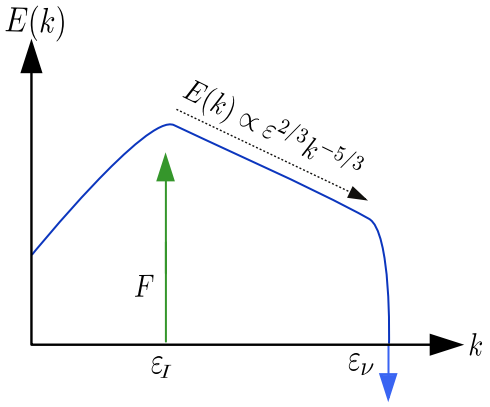

Figure 2. Energy spectrum in 3D turbulence, showing the distribution of energy spectrum $E(k)$ across different wave numbers k with F representing the external forcing. F induces a positive kinetic energy input ϵ_I. All kinetic energy is removed from the system through viscosity, with the output denoted by ϵ_ν.

3D Turbulence The key aspects of Kolmogorov's energy spectrum in three-dimensional turbulence, as shown in Figure 2, can be summarized as follows: Kolmogorov's theory of turbulence introduces the concept of an energy cascade occurring at small length scales, or equivalently, at large wave numbers k. At larger length scales, an external force F injects kinetic energy ϵ_I.
Due to the presence of vortex stretching, represented by $(\boldsymbol{\omega}\cdot\nabla)\boldsymbol{u}$, kinetic energy is transferred to smaller scales at a constant rate ϵ, within a region known as the inertial subrange. At the smallest scales, kinetic energy is dissipated by viscosity. The output of kinetic energy is denoted as ϵ_ν. This smallest scale, typically referred to as the Kolmogorov length scale, falls within the dissipation range. Here, the energy input and output are balanced, creating a statistically stationary state. This process is covered in Kolmogorov's $5/3$ law, which describes the distribution of energy across scales in the inertial subrange.
The distribution of energy across scales is written in the one-dimensional (1D) energy spectrum $E(k)$, defined by the equation

$$E(k) \propto \epsilon^{2/3} k^{-5/3}, \tag{21}$$

where ϵ represents the rate of energy dissipation per unit mass.

2D Turbulence Due to the absence of the vortex stretching term in two-dimensional turbulence, i.e. $(\boldsymbol{\omega}\cdot\nabla)\boldsymbol{u} = 0$ the energy spectrum in the inertial subrange, where enstrophy is conserved, follows a different scaling law than that observed in three-dimensional turbulence (Boffetta & Ecke, 2012). Figure (3) illustrates the energy spectrum $E(k)$ across different wave numbers k. In contrast to three-dimensional turbulence, we have two different outputs for the kinetic energy and enstrophy. The external forcing, F, injects energy and enstrophy into the system, denoted as ϵ_I and ζ_I respectively, to maintain a statistically stationary state. On the one hand, from the length scale of the forcing, the enstrophy is transferred to smaller scales at a constant rate, where it is dissipated by viscosity, ζ_ν, in a process known as the direct enstrophy cascade.

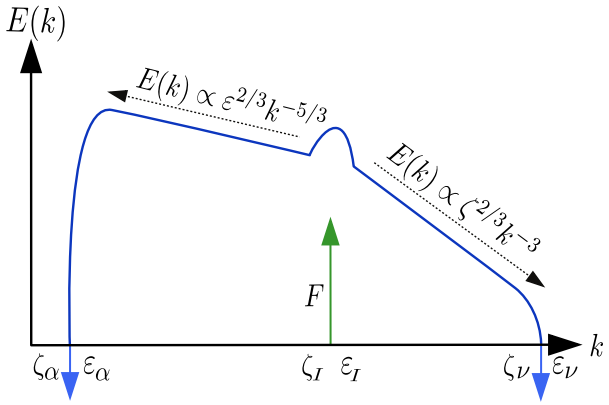

Figure 3. Energy spectrum in 2D turbulence (Laurie, 2019), showing the distribution of energy spectrum $E(k)$ across different wave numbers k with F as the external forcing. F induces a positive enstrophy ζ_I and kinetic energy input ϵ_I. All kinetic energy is removed due to friction at large scales (denoted by ϵ_α), while all enstrophy is dissipated by viscosity ζ_ν at small scales. For analysis purposes, the kinetic energy output at small scales and the enstrophy output at large scales are depicted with ϵ_ν and ϵ_α, respectively, although both are zero.

For the direct enstrophy cascade, $E(k)$ is represented by

$$E(k) \propto \zeta^{2/3} k^{-3}, \tag{22}$$

where ζ is the rate of enstrophy dissipation per unit mass. On the other hand, the kinetic energy is transferred to larger scales at a constant rate from the length scale of forcing, where it is removed by friction, represented as ϵ_α, in a process known as the reverse energy cascade. In this region, the energy spectrum typically follows the classical $-5/3$ scaling law, i.e.

$$E(k) \propto \epsilon^{2/3} k^{-5/3}, \tag{23}$$

where ϵ denotes the rate of energy transfer to larger scales. To better understand the direction of these two cascades, the characteristic length scales are investigated Boffetta & Ecke (2012). The scales characteristic of friction and viscosity are defined as $\ell_\alpha^2 \equiv \epsilon_\alpha/\zeta_\alpha$ and $\ell_\nu^2 \equiv \epsilon_\nu/\zeta_\nu$, respectively. Using a similar relation at the forcing scale, defined as $\ell_I^2 \equiv \epsilon_I/\zeta_I$, one can derive

$$\frac{\epsilon_\nu}{\epsilon_\alpha} = \left(\frac{\ell_\nu}{\ell_I}\right)^2 \left(\frac{\ell_I}{\ell_\alpha}\right)^2 \left(\frac{(\ell_\alpha/\ell_I)^2 - 1}{1 - (\ell_\nu/\ell_I)^2}\right), \tag{24}$$

and

$$\frac{\zeta_\alpha}{\zeta_\nu} = \frac{1 - (\ell_\nu/\ell_I)^2}{(\ell_\alpha/\ell_I)^2 - 1}. \tag{25}$$

For $\ell_\nu \ll \ell_I$, the result for equation (24) is $\epsilon_v/\epsilon_\alpha \to 0$, indicating that all energy flows to large scales in an inverse energy cascade. Conversely, if $\ell_\alpha \gg \ell_I$, then equation (25) yields $\zeta_\alpha/\zeta_\nu \to 0$, implying that all the enstrophy is transferred to small scales in the direct enstrophy cascade.

Energy Spectra in Helical Framework

Investigating energy spectra within helical turbulence reveals behaviors distinct from those observed in the traditional spectrum. Similar to the classical framework, we distinguish two cases.

$u_\eta \neq 0$**:** In this scenario, a Kolmogorov energy spectrum is anticipated, analogous to equation (21). However, the helicity spectrum will vary, depending upon the initial conditions.

$u_\eta = 0$**:** In terms of energy spectra, interesting new cases emerge when $u^\eta = 0$. As $r \to \infty$, the second term on the right-hand side of equation (19) becomes dominant. Scaling analysis indicates that the energy spectrum adopts the following behavior:

$$E(k) \propto \zeta^{2/3}\, k^{-7/3}, \tag{26}$$

where ζ represents the enstrophy flux, and k is the wave number. Conversely, for $r \to 0$, it is not immediately apparent which term on the right-hand side of equation (19) dominate. Nonetheless, dimensional analysis indicates that if the first term dominates, the energy spectrum is similar to that of Kolmogorov given by

$$E(k) \propto \zeta^{2/3}\, k^{-5/3}, \tag{27}$$

and if the second term dominates, the energy spectrum is given as in the classical Cartesian 2D case, i.e.

$$E(k) \propto \zeta^{2/3}\, k^{-3}. \tag{28}$$

ACKNOWLEDGMENT

SA is supported by DFG grant OB $96/56 - 1$ and the Graduate School CE at TU Darmstadt. Both authors are indebted to Johannes Conrad, who has greatly benefited the work in many helpful discussions.

REFERENCES

Abraham, Aliza, Castillo-Castellanos, Andrés & Leweke, Thomas 2023 Simplified model for helical vortex dynamics in the wake of an asymmetric rotor. *Flow* **3**, E5.

Boffetta, Guido & Ecke, Robert E. 2012 Two-dimensional turbulence. *Annual Review of Fluid Mechanics* **44** (1), 427–451.

Bogoyavlenskij, Oleg I. 2000 Helically symmetric astrophysical jets. *Phys. Rev. E* **62**, 8616–8627.

Davidson, P. A. 2004 *Turbulence: An Introduction for Scientists and Engineers*. Oxford University Press.

Delbende, Ivan, Rossi, Maurice & Daube, Oliver 2012 Dns of flows with helical symmetry. *Theoretical and Computational Fluid Dynamics* .

Dierkes, Dominik, Kummer, Florian & Dominik, Plümacher 2021 A high-order discontinuous galerkin solver for helically symmetric flows. *Communications in Computational Physics* **30** (1), 288–320.

Dritschel, David G. 1991 Generalized helical beltrami flows in hydrodynamics and magnetohydrodynamics. *Journal of Fluid Mechanics* **222**, 525–541.

Johnson, J. L., Oberman, C. R., Kulsrud, R. M. & Frieman, E. A. 1958 Some Stable Hydromagnetic Equilibria. *The Physics of Fluids* **1** (4), 281–296.

Kelbin, Olga, Cheviakov, Alexei F. & Oberlack, Martin 2013 New conservation laws of helically symmetric, plane and rotationally symmetric viscous and inviscid flows. *Journal of Fluid Mechanics* **721**, 340–366.

Kundu, P.K., Cohen, I.M. & Dowling, D.R. 2011 *Fluid mechanics: Fifth edition*.

Laurie, Jason 2019 An introduction to 2d turbulence. In *Waves, coherent structures, and turbulence*.

Mitchell, Anthony, Morton, Scott & Forsythe, James 2002 Analysis of delta wing vortical substructures using detached-eddy simulation. *Tech. Rep.* AIAA-2002-2968. United States Air Force Academy, Department of Aeronautics, USAF Academy, CO 80840, USA, approved for public release; distribution unlimited.

Sarpkaya, Turgut 1971 On stationary and travelling vortex breakdowns. *Journal of Fluid Mechanics* **45** (3), 545–559.

Schnack, D. D., Caramana, E. J. & Nebel, R. A. 1985 Three-dimensional magnetohydrodynamic studies of the reversed-field pinch. *The Physics of Fluids* **28** (1), 321–333.

Vermeer, Nord-Jan, Sørensen, Jens & Crespo, Antonio 2003 Wind turbine wake aerodynamics. *Progress in Aerospace Sciences - PROG AEROSP SCI* **39**, 467–510.

Zabielski, L. & Mestel, A. J. 1998 Steady flow in a helically symmetric pipe. *Journal of Fluid Mechanics* **370**, 297–320.